

Synthesis and characterization of a VO^{3+} complex of a pentadentate amine alcohol ligand: towards hydrolytically stable ligands forming model complexes for vanadium-dependent haloperoxidases

Winfried Plass

Fakultät für Chemie der Universität, Lehrstuhl für Anorganische Chemie I, Postfach 100131, D-33501 Bielefeld, Germany

Received 8 May 1995; revised 27 July 1995

Abstract

The vanadium(V) complex of a hydrolytically stable trivalent, pentadentate amine alcohol ligand has been synthesized by reaction with ammonium *meta*-vanadate. The ligand was prepared by reduction of the Schiff base precursor *N*-salicylidene-2-(bis(2-hydroxyethyl)amino)ethylamine and exhibits an enlarged flexibility as compared to its Schiff base analogue. The vanadium(V) complex is characterized by ^1H , ^{13}C and ^{51}V NMR, vibrational (IR, Raman and resonance Raman) and electronic spectroscopy. The LMCT transition of the complex has been assigned on the basis of resonance Raman spectroscopy and density functional calculations (LDA). The X-ray crystal structure analysis of $\text{C}_{13}\text{H}_{19}\text{N}_2\text{O}_4\text{V}$ (monoclinic, space group $C2/c$: $a = 1948.1(4)$, $b = 1184.9(2)$, $c = 1328.3(2)$ pm, $\beta = 114.86(1)^\circ$, $Z = 8$) shows that the vanadium(V) center has a distorted octahedral environment with the oxo group in the *trans* position to the tertiary amine nitrogen. In the solid state racemic pairs of the vanadium(V) complex are formed by hydrogen bridges ($\text{N}-\text{H}\cdots\text{O}$). The bond valence sum (BVS) analysis is applied to the complex prepared in this work and compared with the results obtained for a series of more than twenty relevant six-coordinate complexes. In solution a second isomer with the oxo group *trans* to the secondary amine nitrogen is observed. The ratio of the two isomers varies with the solvent, as was determined by ^{51}V NMR spectroscopy. The methanolysis as well as hydrolysis reaction of the vanadium(V) complex is studied by ^{51}V NMR. The implications of the results for the proposed model of the active site of vanadium-dependent haloperoxidases are discussed.

Keywords: Crystal structures; Vanadium complexes; Polydentate amine alcohol complexes

1. Introduction

The increasing interest in the coordination chemistry of vanadium stems from its recognized relevance in a wide variety of biological systems [1–4]. Vanadium is found in the natural product amavadin isolated from the mushroom *Amanita muscaria* [5] and in ascidian blood cells [6]. Moreover, vanadate is known as a potent inhibitor of phosphate metabolism [7,8] and as an insulin mimetic [9]. To date, two enzymes dependent on vanadium for activity are identified and characterized. The vanadium nitrogenase isolated from *Azotobacter chroococcum* [10], which catalyzes the reduction of dinitrogen to ammonia, was a challenge for the microbiology, since molybdenum was considered as an essential component of nitrogenases [11,12]. Vanadium-dependent haloperoxidases, which catalyze the oxidative halogenation of a large variety of organic compounds, have been isolated from several red and brown algae as well as lichen [13–17].

The active site of vanadium-dependent haloperoxidases consists of a vanadium(V) center in an oxygen and nitrogen rich donor environment. Based on a wide variety of physical measurements on the native and the reduced enzyme, a model for the active site has been proposed (XAS [18,19], ^{51}V NMR [20,21] and ESR spectroscopy [22–24]). In this model a VO^{3+} core (V–O 161 ppm) is coordinated to at least four, probably five, oxygen and nitrogen donors (3×172 ppm and 2×211 ppm). Even a seven-coordinate vanadium center has been proposed on the basis of the chemical shift observed in the ^{51}V NMR spectrum of the native enzyme [20]. These studies also indicated that the vanadium center does not undergo redox cycling during turnover, which is in marked contrast to the widely distributed heme peroxidases [25].

Little is known about the coordination chemistry of VO^{3+} with biologically relevant oxygen/nitrogen donor sets. The commonly utilized Schiff base ligands generally lack hydrolytic stability due to their imino functionality [26]. On the

other hand, a ligand system utilized for model compounds should not yield highly stable VO^{3+} chelate complexes, which in turn are not expected to possess catalytic activity. Therefore, it is important to explore the coordination chemistry of hydrolytically stable ligands that provide a mixed oxygen/nitrogen donor set with potentially semi-labile functionalities. An example for such a ligand is readily available from the earlier reported Schiff base ligand *N*-salicylidene-2-(bis(2-hydroxyethyl)amino)ethylamine (H_3sabhea) [27].

2. Experimental

2.1. Materials

Abbreviations used throughout the text: H_3sabhea = *N*-salicylidene-2-(bis(2-hydroxyethyl)amino)ethylamine; $\text{H}_3\text{Mesabhea}$ = *N*-(1-(2-hydroxyphenyl)ethylidene)-2-(bis(2-hydroxyethyl)amino)ethylamine; H_3hebab = 1,1-bis(2-hydroxyethyl)-4-(2-hydroxybenzyl)-1,4-diazabutane. The Schiff base precursor H_3sabhea was prepared as previously described [27]. All other chemicals were of reagent grade.

2.2. Instrumentation

^1H , ^{13}C , ^{51}V , $^1\text{H}\{^1\text{H}\}$ COSY and $^1\text{H}\{^{13}\text{C}\}$ heteronuclear correlation NMR spectra were recorded on Bruker AM300 (^{51}V , 78.906 MHz) and AC250 (^1H , 250.133 MHz; ^{13}C 62.896 MHz) spectrometers, respectively. Chemical shifts in ppm are reported as δ downfield from the standards, tetramethylsilane (^1H and ^{13}C) and VOCl_3 (^{51}V). IR spectra were recorded on Mattson Polaris and Bruker IFS66 FT-IR spectrometers. Raman spectra (solid state and DMF solution) were measured with a Bruker IFS66/FRA106 spectrometer ($\lambda_e = 1064$ nm) and resonance Raman spectra on a Spex Ramalog 5 spectrometer ($\lambda_e = 514.5$ nm). UV-Vis spectra were recorded on Beckman Acta MIV (solid state reflection, cellulose as calibration standard) and Shimadzu UV-160A spectrometers (solution transmission).

2.3. Synthesis

2.3.1. H_3hebab

To a solution of H_3sabhea (3.27 g, 13.0 mmol) in 40 ml ethanol at r.t. was added NaBH_4 (0.80 g, 21.1 mmol) in small portions over 30 min. After the addition was complete, the reaction mixture was stirred at r.t. for an additional 12 h and subsequently refluxed for 2 h. The solvent was removed under reduced pressure, and to the residue was added 25 ml of an aqueous NH_4Cl (2.5 g) solution. The mixture was extracted with chloroform (3×50 ml). The combined organic fractions were washed with water, and dried over anhydrous sodium sulfate. The mixture was filtered, and the chloroform removed under reduced pressure to afford a viscous yellow

oil, which slowly crystallized upon standing at r.t. Yield: 2.80 g (85%); m.p. 73–75 °C. ^1H NMR (DMSO- d_6): 2.57 (t, 4H, $\text{NCH}_2\text{CH}_2\text{OH}$, $^3J(\text{HH}) = 6.0$ Hz), 2.62 (m, 4H, $\text{NCH}_2\text{CH}_2\text{NH}$), 3.47 (t, 4H, $\text{NCH}_2\text{CH}_2\text{OH}$, $J = 6.0$ Hz), 3.85 (s, 2H, NHCH_2Ph), 5.62 (s, 4H, OH/NH), 6.68–6.74 (m, 2H, Ph), 7.06–7.21 (m, 2H, Ph). ^{13}C NMR (DMSO- d_6): 46.1 ($\text{NCH}_2\text{CH}_2\text{NH}$), 50.1 (NHCH_2Ph), 54.0 ($\text{NCH}_2\text{CH}_2\text{NH}$), 56.9 ($\text{NCH}_2\text{CH}_2\text{OH}$), 59.2 ($\text{NCH}_2\text{CH}_2\text{OH}$), 115.5, 117.7 (Ph), 124.1 (Ph, *ipso*-C{ CH_2NH }), 127.6, 128.3 (Ph), 158.1 (Ph, *ipso*-C{OH}). IR (KBr pellet, cm^{-1}): 3250 (br,m, $\nu(\text{N-H})$). UV-Vis (CHCl_3 solution, ν_{max} in 10^3 cm^{-1} (ϵ in $10^6 \text{ cm}^2 \text{ mol}^{-1}$): 41.3 (5.8), 36.2 (4.6).

2.3.2. $\text{VO}(\text{hebab})$

NH_4VO_3 (0.40 g, 3.4 mmol) was added to a solution of H_3hebab (0.87 g, 3.4 mmol) in 30 ml methanol. The resulting mixture was heated under reflux for 3 h. The hot reaction mixture was filtered to remove unreacted NH_4VO_3 . Upon cooling the filtrate to r.t. red crystals of the product formed. Reduction of the solution volume to about one-third afforded a second crop of product. Total yield: 0.67 g (62%); m.p. > 225 °C (dec.). Anal. Calc. for $\text{C}_{13}\text{H}_{19}\text{N}_2\text{O}_4\text{V}$ (318.25): C, 49.06; H, 6.02; N, 8.80. Found: C, 49.21; H, 6.04; N, 8.68%. ^1H NMR (DMSO- d_6): 2.37–2.61 (m, 3H, $\text{NCH}_2\text{CH}_2\text{NH}$), 2.82–2.91 (m, 2H, $\text{NCH}_2\text{CH}_2\text{OV}$), 3.08–3.27 (m, 3H, $\text{NCH}_2\text{CH}_2\text{NH}$, $\text{NCH}_2\text{CH}_2\text{OV}$), 3.80 (d, 1H, PhCH_2NH , $^2J(\text{HH}) = 12.9$ Hz), 4.39–4.50 (m, 2H, PhCH_2NH , $\text{NCH}_2\text{CH}_2\text{OV}$), 4.64–4.87 (m, 3H, $\text{NCH}_2\text{CH}_2\text{OV}$), 6.29 (s, 1H, NH), 6.54–6.61 (m, 2H, Ph), 7.02–7.09 (m, 2H, Ph). ^{13}C NMR (DMSO- d_6): 51.5 ($\text{NCH}_2\text{CH}_2\text{NH}$), 55.9 ($\text{NCH}_2\text{CH}_2\text{NH}$), 56.5 (PhCH_2NH), 57.2 ($\text{NCH}_2\text{CH}_2\text{OV}$), 59.3 ($\text{NCH}_2\text{CH}_2\text{OV}$), 74.7 ($\text{NCH}_2\text{CH}_2\text{OV}$), 76.5 ($\text{NCH}_2\text{CH}_2\text{OV}$), 117.2 (Ph), 117.8 (Ph), 121.7 (Ph, *ipso*-C{ CH_2NH }), 129.1 (Ph), 130.0 (Ph), 164.1 (Ph, *ipso*-C{OV}). ^{51}V NMR data: see Section 3 and Table 4. IR (KBr pellet, cm^{-1}): 3095 (br,m, $\nu(\text{N-H})$); 952 (vs, $\nu(\text{V=O})$). Raman ($\lambda_e = 1064$ nm, 30 mW, powder on Al support, cm^{-1}): 950 (vs, $\nu(\text{V=O})$). Solution Raman ($\lambda_e = 1064$ nm, 200 mW, saturated DMF solution, cm^{-1}): 960 ($\nu(\text{V=O})$). UV-Vis (solid state reflection, ν_{max} in 10^3 cm^{-1}): 32.0 (sh), 25.0, 19.5 (sh). UV-Vis (CHCl_3 solution, ν_{max} in 10^3 cm^{-1} (ϵ in $10^6 \text{ cm}^2 \text{ mol}^{-1}$): 41.0 (7.1), 38.2 (7.0), 35.1 (sh), 27.5 (3.1), 22.5 (sh).

2.4. X-ray structure analysis of $\text{VO}(\text{hebab})$

The crystallographic data were collected on a Siemens P2₁ four-circle diffractometer (graphite monochromatized Mo $\text{K}\alpha$ radiation; 71.073 pm). The final unit-cell parameters were obtained by least-squares fitting of the setting angles for 19 reflections with 2θ between 18 and 30°. A summary of crystallographic data and data collection for $\text{VO}(\text{hebab})$ is given in Table 1. The intensities of three standard reflections, measured every 97 reflections throughout the data collection, did not show any decay. The data was semi-empirically corrected for absorption effects based on azimuthal scans for ten

Table 1
Summary of crystallographic data and data collection for VO(hebab)

Formula	C ₁₃ H ₁₉ N ₂ O ₄ V
Formula weight	318.25
Crystal size (mm)	0.35 × 0.30 × 0.20
Crystal system	monoclinic
Space group	C2/c (No. 15 [28])
Lattice parameters	
<i>a</i> (pm)	1948.1(4)
<i>b</i> (pm)	1184.9(2)
<i>c</i> (pm)	1328.3(2)
β (°)	114.86(1)
Cell volume (10 ⁶ pm ³)	2782.0(8)
Z	8
Temperature (K)	293
D _{calc} (g cm ⁻³)	1.520
F(000)	1328
μ(Mo Kα) (mm ⁻¹)	0.728
Data collection range (°)	4 < 2θ < 50
Reflection array	+ <i>h</i> , + <i>k</i> , ± <i>l</i>
Scan type, scan width (°)	ω-scan, 1.4
Reflections measured	
total	2525
unique	2449 (<i>R</i> _{int} = 0.0304)
observed	1565 (<i>F</i> > 4σ(<i>F</i>))
Reflections used in refinement (<i>N_r</i>)	2417
No. variables (<i>N_p</i>)	257
Goodness-of-fit <i>s</i> ^a on <i>F</i> ²	1.064
<i>R</i> ₁ ^b	0.051
<i>wR</i> ₂ ^c	0.100
δρ: min., max. (× 10 ⁻⁶ e pm ⁻³)	-0.3; 0.3

$$^a s = \sqrt{\sum w(F_o^2 - F_c^2)^2 / (N_r - N_p)}$$

$$^b R_1 = \sum ||F_o| - |F_c|| / \sum |F_o|; \text{calculated for all observed reflections.}$$

$$^c wR_2 = \sqrt{\sum w(F_o^2 - F_c^2)^2 / \sum w(F_o^2)^2} \text{ with } w^{-1} = \sigma^2(F_o^2) + (0.016P)^2 + 7.0P \text{ and } P = 1/3 (\text{max.}(0, F_o^2) + 2F_c^2); \text{calculated for all reflections used in refinement.}$$

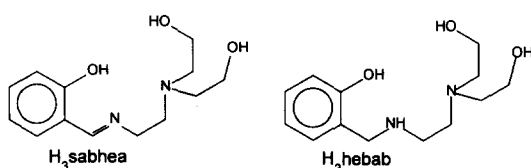


Fig. 1. Schematic drawing of the pentadentate amine alcohol ligand used in this study and its corresponding Schiff base. (For abbreviations see text.)

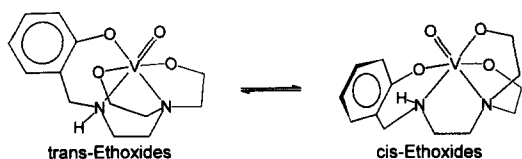


Fig. 2. Representation of the two isomers of VO(hebab). The *cis*-ethoxide isomer on the right is the crystallographically characterized species.

reflections. The structure was solved by direct methods (SHELXTL-PLUS) [29] and subsequent least-squares refinement of the function $\sum w(F_o^2 - F_c^2)^2$ (SHELXL-93) [30]. All non-hydrogen atoms were refined with anisotropic displacement parameters. Hydrogen atoms were located from the difference Fourier map and refined with isotropic displacement parameters.

3. Results and discussion

3.1. Synthesis

The synthetic goal was to establish a hydrolytically stable, high-denticity ligand donor set and subsequently to introduce this flexible ligand system into the complex chemistry of vanadium. Such ligand systems which contain also potentially pendant functional groups are important for structural and mechanistic model studies on the vanadium-dependent haloperoxidase systems. Schiff base ligands of the H₃sabhea type have already been shown to form mono-oxovanadium(V) complexes that are stable against hydrolysis in methanol solution [27]. Nevertheless, Schiff base ligands are usually sensitive to hydrolysis in aqueous media, especially under acidic or basic conditions as well as in the presence of peroxides. Starting from the Schiff base H₃sabhea the pentadentate amine-phenol alkoxide ligand H₃hebab is synthesized by reduction with NaBH₄ (see Fig. 1). Recently, another synthetic approach to the H₃hebab ligand system (with a lower overall yield) has been reported, but attempts to isolate the corresponding vanadium(V) complex were unsuccessful [31]. Due to the reduction of the carbon-nitrogen double bond the H₃hebab ligand is more flexible than its Schiff base analogue and, therefore, the preference of the *trans* coordination mode of the phenolate oxygen with respect to the tertiary amine nitrogen observed for VO(sabhea) type complexes [27] is diminished. Thus, the H₃hebab ligand can form two isomeric coordination pockets, i.e. a *cis*- or *trans*-oid conformation of the phenolate oxygen and the tertiary amine nitrogen (cf. Fig. 2).

Ammonium *meta*-vanadate reacts with a refluxing methanol solution of H₃hebab to form the mono-oxovanadium(V) complex VO(hebab). As was already observed in the synthesis of the VO(sabhea) type complexes [27], the H₂O formed by the reaction does not cause any hydrolysis. Moreover, the VO(hebab) complex isolated as red-brown prismatic crystals can be stored in air over a period of months without any measurable decomposition (for solution stability see Section 3.3.). An alternative synthetic approach is the reaction of oxovanadium(V) trimethoxide with the H₃hebab ligand in chloroform or methanol solution. Oxovanadium(V) methoxide species can also be regarded as reactive intermediates in the reaction of ammonium *meta*-vanadate with the free ligand in refluxing methanol (*vide infra*).

3.2. Description of the structure of VO(hebab)

The mono-oxovanadium(V) complex VO(hebab) depicted in Fig. 3 crystallizes as a racemic mixture of its two enantiomeric forms in the centrosymmetric monoclinic space group C2/c. The fractional atomic coordinates and isotropic displacement parameters for the non-hydrogen atoms in VO(hebab) are listed in Table 2, and selected bond lengths and angles for VO(hebab) are given in Table 3. The crystal structure reveals that in the solid state only one of the two

potential coordination modes of the H₃hebab ligand is actually realized. In fact, it is important to note that the reflection pattern of the measured and calculated powder diffraction diagram is in agreement, with the latter based on the single crystal data. Thus, the isolated solid material of the complex VO(hebab) consists solely of the crystallographically characterized isomer. In this isomer the tertiary amine nitrogen (N2) is coordinated *trans* to the oxo group and the ethanolate oxygens (O3, O4) are oriented *cis* to each other (see Fig. 2). In contrast, for the corresponding Schiff base ligand the oxo group is found to coordinate *trans* to the imine nitrogen and, moreover, the phenolate oxygen, imine nitrogen and amine nitrogen atoms form a meridional chelate [27]. The slightly distorted octahedral coordination sphere around the vanadium center consists of the pentadentate hebab³⁻ ligand (N1, N2, O2, O3 and O4) and a terminal oxo moiety (O1), with dihedral angles formed by the equatorial mean least-squares planes of 88.8, 89.1 and 89.3°. The largest deviations of the vanadium atom from these mean planes are consistent with a displacement towards the octahedral edge formed by the terminal oxo ligand (O1) and the ethanolate oxygen (O3) *trans* to the secondary amine nitrogen.

The vanadium to terminal oxo group (O1) distance in VO(hebab) is 159.5 pm which is slightly shorter than the V=O bond (161.2 pm) in the vanadium complex with the corresponding Schiff base, the derivative with the methyl substitution at the imine carbon atom, VO(Mesabhea) [27]. This can be attributed to a weaker donor ability of the tertiary amine nitrogen in VO(hebab) compared to the imine nitrogen in VO(Mesabhea). Consistently, the V–N2 distance in VO(hebab) is elongated to 230.9 pm, a value close to that reported for a similar pentadentate bisphenolate ligand (231.3 pm) [31]. One of the vanadium to ethanolate oxygen distances (V–O3, 182.2 pm), although close to the upper limit, is within the usually observed range for vanadium alkoxide bonds in six-coordinate complexes (172–184 pm) [31–38]. The second ethanolate (O4) to vanadium distance is significantly longer at 188.5 pm. This is not unexpected since the respective *trans* positions are occupied by two distinctively different donor atoms, a secondary amine nitrogen (N1) and a phenolate oxygen (O2). Thus, the vanadium–phenolate oxygen distance is substantially elongated (V–O2,

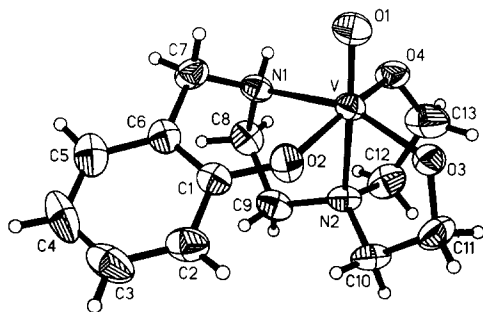


Fig. 3. Molecular structure and numbering scheme for VO(hebab). Thermal ellipsoids of non-hydrogen atoms are drawn at 50% probability, and hydrogen atoms with arbitrary radii.

Table 2

Fractional atomic coordinates ($\times 10^4$) and equivalent isotropic displacement parameters U_{eq} ($\text{pm}^2 \times 10^{-1}$) for the non-hydrogen atoms in VO(hebab)

	<i>x/a</i>	<i>y/b</i>	<i>z/c</i>	U_{eq}^a
V	2571(1)	888(1)	1406(1)	31(1)
O1	2174(2)	1932(3)	1705(3)	51(1)
O2	1938(2)	-317(3)	1424(2)	42(1)
O3	3312(2)	369(2)	2696(2)	39(1)
O4	3220(2)	1777(2)	1007(3)	43(1)
N1	1851(2)	888(3)	-340(3)	34(1)
N2	3149(2)	-441(3)	750(3)	36(1)
C1	1322(2)	-858(4)	729(3)	35(1)
C2	1145(3)	-1923(4)	1030(5)	46(1)
C3	516(3)	-2502(5)	321(6)	60(2)
C4	50(3)	-2043(5)	-677(6)	64(2)
C5	221(3)	-1007(5)	-995(4)	52(1)
C6	854(2)	-407(4)	-298(3)	37(1)
C7	1037(3)	729(4)	-618(4)	40(1)
C8	2133(3)	142(4)	-998(4)	43(1)
C9	2574(3)	-854(4)	-323(4)	43(1)
C10	3389(3)	-1281(4)	1650(4)	44(1)
C11	3700(3)	-660(5)	2754(4)	49(1)
C12	3785(3)	116(5)	626(5)	53(1)
C13	3910(3)	1284(5)	1143(7)	69(2)

^a Equivalent isotropic U_{eq} are defined as one-third of the trace of the orthogonalized U_{ij} tensor.

Table 3

Selected bond lengths (pm) and angles (°) for VO(hebab)

V–O1	159.5(3)	V–O4	188.5(3)
V–O2	189.2(3)	V–N1	214.7(3)
V–O3	182.2(3)	V–N2	230.9(3)
O1–V–O2	101.3(2)	O3–V–N1	156.30(14)
O1–V–O3	107.6(2)	O4–V–N1	84.68(14)
O1–V–O4	95.1(2)	O1–V–N2	170.8(2)
O2–V–O3	89.79(13)	O2–V–N2	85.12(13)
O2–V–O4	160.53(13)	O3–V–N2	78.78(13)
O3–V–O4	95.35(13)	O4–V–N2	77.52(13)
O1–V–N1	96.0(2)	N2–V–N1	78.10(13)
O2–V–N1	83.15(14)		

189.2 pm) compared to the Schiff base complex VO(Mesabhea) (183.7 pm [27]).

It is an intriguing fact that no six-coordinate vanadium(V) complex is reported in the literature that resembles the vanadium environment proposed on the basis of EXAFS data¹ of the native bromoperoxidase enzyme from *Ascophyllum nodosum* [19]. In this model for the active site the vanadium(V) is coordinated by two nitrogen or oxygen donors at 211 pm, three oxygen ligands at 172 pm and an oxo group at 161 pm. Both complexes the VO(hebab) as well as the Schiff base analogue VO(Mesabhea) [27] possess a six-coordinate N₂O₄ environment for the vanadium center with an oxo ligand

¹ Metal–ligand bond lengths obtained from the analysis of EXAFS data are generally in good agreement with the distances determined from X-ray crystallographic data for both metalloproteins and transition metal complexes [39].

and one of the nitrogen donors at the desired bond lengths, whereas the second V–N bond *trans* to the oxo group is considerably elongated in both cases (VO(hebab) 230.9, VO(Mesabhea) 227.1 pm). Also the three V–O bonds in both complexes are significantly longer than the reported EXAFS distance of 172 pm. However, thus far only two six-coordinate vanadium(V) complexes have been reported with a vanadium(V) to oxygen bond at the desired value of about 172 pm [32].

To this end the bond valence sum analysis (BVS) [40,41] based on the parameters reported by Brown and Altermatt [42] provides a valuable tool. Its applicability to metalloenzymes and related model complexes has already been demonstrated [39]. The expression used to calculate the bond valence for a particular bond is given in Eq. (1), where B (37 pm) and r_0 are empirically determined parameters.

$$s_{ij} = \exp\left(\frac{r_0 - r_{ij}}{B}\right) \quad (1)$$

The bond valence sum V_i for an individual atom, which can usually be related to its oxidation state, is calculated according to Eq. (2).

$$V_i = \sum_j s_{ij} \quad (2)$$

The values for r_0 not tabulated in Ref. [42] can be calculated according to a simple formula parameterized for a wide variety of atom pairs [42]. The values of r_0 for the relevant atom pairs are: V^v–O = 180.3 pm and V^v–N = 187.5 pm.

It is important to probe the reliability of the BVS approach in the analysis of six-coordinate mono-oxovanadium(V) complexes with a mixed nitrogen/oxygen environment, as they are potential model compounds for the active site of vanadium-dependent haloperoxidases. The BVS's calculated for a series of more than 20 relevant complexes [31,33–38,43–50] range from 4.9 to 5.2 with an average of 5.10 which is in good agreement with the oxidation state of the vanadium. As the rather large average value already indicates most of the BVS's are within a small range of 5.10 ± 0.05 . The BVS's calculated for VO(hebab) and the Schiff base analogue VO(Mesabhea) [27] are 5.09 and 5.11, respectively, and can be regarded as typical for this class of complexes. On the other hand there are exceptions which do not fit in the given range. The rather low BVS's calculated for these vanadium(V) complexes (4.6 to 4.7) are probably due to the non-innocent character of some of the coordinated ligands, such as catechol [51,52].

As was already shown in a recent EXAFS study [32], the V–O and V–N bond length values determined from EXAFS data of the native bromoperoxidase [19] are not consistent with the originally proposed six-coordinate structure for the active site. An alternative model based on the exceptional high-field ⁵¹V NMR chemical shift observed for the native enzyme even discusses a seven-coordinate vanadium(V) center with a carboxylate-rich coordination environment [20]. Although one has to be aware of the limitations of the

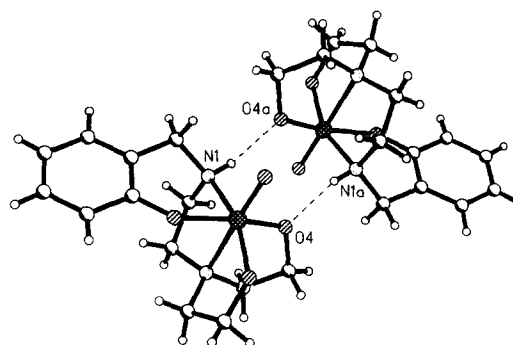


Fig. 4. Representation of the hydrogen bonds between two enantiomers of VO(hebab) in the crystal structure.

BVS model, especially when its correlation to the oxidation state of the particular metal center is considered, the calculated BVS of 6.5 for a six-coordinate environment (one V=O at 163 pm, three V–O at 172 pm, and two V–N at 211 pm) is considerably above the expected range². Therefore, a six- or even higher-coordinate structure for the active site seems to be unlikely (cf. Ref. [32]), and for the most probable combinations of a five-coordinate structure, where one of the three proposed rather short V–O bonds is dismissed, BVS values of about 5.2 are calculated. Finally, it is important to note that further testing of the applicability of the BVS method and, in particular, its correlation to the oxidation state is needed, especially to probe the effects of ligands with unusual electronic and steric properties.

The crystal structure of VO(hebab) exhibits a short intermolecular contact between the imine nitrogen atom (N1) and the ethanolate oxygen (O4) of two neighboring molecules with a distance of 289 pm. As a result a hydrogen bridged racemic dimer is formed in the solid state (see Fig. 4). This hydrogen bonding certainly contributes to the elongation of the V–O4 bond (vide supra). The packing of the [VO(hebab)]₂ dimers in the crystal structure is illustrated in the unit cell diagram of Fig. 5. It shows that the hydrogen bonds are approximately aligned along the crystallographic *b*-axis.

3.3. Spectroscopic studies

While the X-ray diffraction experiments clearly show that VO(hebab) in its solid state is only comprised of one possible isomeric form (cf. Fig. 2), complementary techniques are necessary to probe the solution structure of the complex. There are two questions of crucial importance related to the solution behavior of such complexes, namely their integrity and the retainment of their solid state structure. This is of particular interest for complexes intended to serve as structural or functional models for biologically relevant systems. For vanadium(V) complexes ⁵¹V and ¹³C NMR spectroscopy can be a very efficient tool [53–57].

² For metalloenzyme model complexes the BVS values calculated on the basis of EXAFS data are generally even lower than those obtained from X-ray crystallographic data [39].

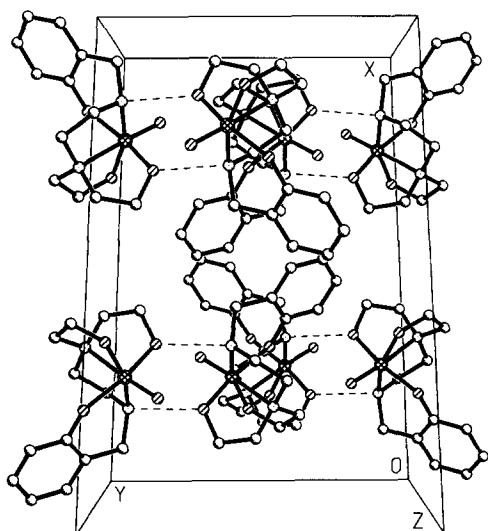


Fig. 5. Packing diagram of VO(hebab). The hydrogen bonds between pairs of enantiomers are indicated by broken lines.

According to the ^{51}V NMR data two isomers are present in solutions of VO(hebab) (see Table 4 and Fig. 2). The rather low solubility of VO(hebab) in the appropriate organic solvents does not permit the observation of the ^{13}C resonances of the minor isomer. Moreover, most of the ^1H resonances of the minor isomer are hidden under the spectral lines of the major species observed in solution. Consequently, only the ^1H and ^{13}C NMR data for the major isomer can be evaluated. The data assigned on the basis of $^1\text{H}\{^1\text{H}\}$ COSY, APT ^{13}C , and $^1\text{H}\{^{13}\text{C}\}$ heteronuclear correlation NMR spectra are summarized in Section 2.

The ^{13}C NMR spectrum is in agreement with a pentadentate ligand formulation in solution. In addition, the two observed distinctively different sets of resonances for the two ethoxide chelate rings support the *cis*-ethoxide formulation for the major solution isomer, which therefore corresponds to the crystallographically characterized isomer (vide infra). All ^{13}C resonances of the H₃hebab ligand, except those of the unsubstituted phenyl carbon atoms, undergo marked downfield shifts upon formation of the vanadium(V) complex. This coordination effect is most pronounced for the resonances of the alcohol carbons, which are shifted by more than 15 ppm downfield. For the corresponding Schiff base complex similar effects on the ^{13}C resonances have been observed [27]. According to the assignment of the ^1H resonances all protons of the major isomer are chemically different. In this context it is worth noting that for the minor isomer two ^1H resonances downfield from 5 ppm (5.03 and 5.36 ppm) are observed, which can be attributed to protons attached to the alcohol carbons. In fact, these resonances appear at shift values similar to that observed for the most downfield set of the diastereotopic methylene protons (5.65 ppm) in the related vanadium(V) Schiff base complex [27]. This further supports the assignment of the species with the two ethoxides oriented *trans* to each other as the minor isomer observed in solution (see Fig. 2).

Table 4

^{51}V NMR data for VO(hebab) in different organic solvents ^a (for notation and structure of the two isomers see Fig. 2)

Solvent	<i>trans</i> -Ethoxides	<i>cis</i> -Ethoxides	Ratio (<i>cis/trans</i>)
DMSO	−425(310)	−448(470)	12
DMF	−430(150)	−451(220)	8
CHCl ₃	−437(150)	−449(310)	1.25
MeOH ^b	−440(140)	−460(220)	4

^a Shifts in ppm; line widths at half-height ($\Delta\nu_{1/2}$ in Hz) are given in parentheses.

^b In methanol solution two additional resonances at −492(110) and −554(80) are observed with relative integrals (based on the *trans* isomer) of 2 and 0.25, respectively.

The ^{51}V NMR data for VO(hebab) summarized in Table 4 show that the ratio of the two isomers (see Fig. 2) is strongly dependent on the nature of the organic solvent. The ratio of *cis* to *trans* ethanolate isomer concomitantly increases with the dipolar character of the solvent, and the resonance of the *cis* isomer is generally observed 12–23 ppm upfield.

The ^{51}V chemical shift of the crystallographically characterized *cis* isomer is observed at −450 ppm for aprotic solvents (DMSO, DMF and CHCl₃), whereas in methanol solution the resonance is shifted upfield by 10 ppm. In contrast, a pronounced solvent dependency for the second resonance related to the *trans* isomer is already found within the series of aprotic solvents.

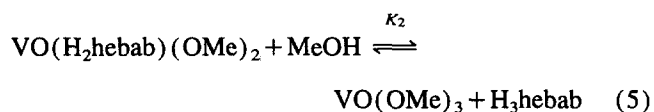
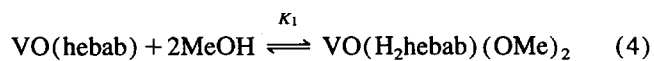
Additional proof for the given assignment of the ^{51}V resonances is evident from the respective line widths at half-height since they are related to both dynamic and structural features of the complexes. The line width at half-height, $\Delta\nu_{1/2}$, for a quadrupolar nucleus is given by Eq. (3), where I is the nuclear spin and τ_r is the rotational correlation time [55].

$$\Delta\nu_{1/2} = \frac{\pi}{10} \frac{2I+3}{I^2(2I-1)} \chi^2(3+\eta^2)\tau_r \quad (3)$$

The asymmetry parameter $\eta = (V_{xx} - V_{yy})/V_{zz}$ is determined by the principal components of the diagonalized electric field gradient (EFG) tensor ($0 < \eta < 1$) and $\chi = e^2QV_{zz}/h$ is the quadrupole coupling constant, in which eQ is the quadrupole moment. The quadrupole moment eQ as well as the rotational correlation time τ_r , which is dependent on the size of the complex in solution, should be about the same for both isomers. Thus, the differences of the line widths observed for the two isomers can only be related to variations of the principal components of the EFG (V_{zz} and η) and, hence, the symmetry of the ligand field. According to the significantly enhanced line width observed for the upfield resonance in all solvents, this resonance has to be assigned to the isomer with lower symmetry (larger η), which is the one with the tertiary amine nitrogen *trans* to the oxo group (cf. Fig. 2). It should be noted that the line widths are also generally sensitive to exchange processes. However, as VT ^{51}V NMR shows the interconversion between the two isomers

at room temperature is at the slow exchange limit as compared to the time scale of the NMR experiment and, moreover, is expected to similarly influence both resonances.

In methanol solutions of VO(hebab) two additional complexes are detected by ^{51}V NMR spectroscopy (see Table 4). The major species observed is VO(hebab) in its two isomeric forms. The resonance of the first additional complex appears at -492 ppm and the second is identified as oxovanadium(V) trimethoxide according to its resonance at -554 ppm.



The complex assigned to the resonance at -492 ppm is presumably a reaction product between VO(hebab) and two molecules of methanol, as shown in Eq. (4). This assumption is consistent with the difference in basicity of the ethoxide and phenolate oxygens, and is further supported by the fact that in contrast to VO(hebab) only one ^{51}V resonance is observed attributable to this intermediate species. There are basically three possible structures for the intermediate complex derived according to Eq. (4), two octahedral (cf. Fig. 2) and one penta-coordinate arrangement. The observed ^{51}V NMR chemical shift of -492 ppm is consistent with both a five-coordinate and six-coordinate vanadium(V) complex. The limited solubility in methanol together with the small formation constant of the VO(H₂hebab)(OMe)₂ complex (vide infra) prevented its characterization by ^{13}C NMR spectroscopy. Based on a recently proposed empirical relationship between the ^{51}V NMR chemical shift and the corresponding line width at half-height [57] the sharp resonance ($\Delta\nu_{1/2} = 110$ Hz; cf. Table 4) observed for the intermediate complex suggests a penta-coordinate environment for the vanadium(V) center. Nevertheless, this empirical relationship has its limitations, as it is only tested for a specific type of ligands [57]. In this context it is important to note that some of the line widths observed for the six-coordinate complexes derived from H₃sabhea type ligands [27] as well as VO(hebab) (see Table 4) are already in the range given for those complexes characterized as five-coordinate by the aforementioned empirical relationship (given range for solutions in water: $\Delta\nu_{1/2} = 130$ – 180 Hz [57]). Moreover, additional care has to be taken with respect to the applied solvent (cf. Table 4), as especially water seems to enhance the observed line widths (vide infra).

The equilibrium constants $K_1 = 7 \times 10^{-4} \text{ M}^{-2}$ and $K_2 = 6 \times 10^{-6}$ for the reactions according to Eqs. (4) and (5) are calculated on the basis of the integration in the ^{51}V NMR spectra. The constants were obtained by either approaching the equilibrium in methanol solution of VO(hebab) or in solutions with equimolar amounts of oxovanadium(V) trimethoxide and H₃hebab. The equilibrium constant K_2 is

indicative for the pronounced stability of the phenolate substituted oxovanadium(V) ester with respect to the trimethoxide starting material. However, the predominant species in methanol solution are the two isomers of the VO(hebab) complex depicted in Fig. 2.

To address the stability of the VO(hebab) complex in biologically relevant protic media a series of ^{51}V NMR spectra in water/DMSO mixtures with variable water content (up to a ratio in volume of 1.0) was measured at total vanadium concentrations ranging from 25 to 50 mM. In DMSO solution only the resonances attributed to the two isomers of VO(hebab) are observed. For solutions containing water a significant increase for the line width of the resonances related to the two VO(hebab) isomers (-425 ppm: 350 Hz; -448 ppm: 540 Hz) is observed (cf. Table 4). In solutions with a water/DMSO ratio up to 0.1 the resonances observed for the two isomers account for more than 90% of the total vanadium concentration and no additional distinct resonance is observed in the ^{51}V NMR spectra. Resonances attributable to the remaining vanadium content can only be identified by integration and appear in the range between -540 and -600 ppm. Upon increasing the water content to ratios of 0.25, 0.4, 0.7 and 1.0 new resonances are observed at -579 and -588 ppm (oligomeric vanadate species [54]), but still more than 80, 70, 50 and 30%, respectively, of the vanadium content can be identified as intact VO(hebab) complex. Although the overall solubility of VO(hebab) in water is rather low, even under these conditions 10% of the vanadium detected in solution by ^{51}V NMR spectroscopy are observed as unhydrolysed VO(hebab) complex. It is interesting to note that there is no ^{51}V NMR spectroscopic evidence for the formation of a VO₂(H₂hebab) pervanadyl complex as hydrolysis intermediate, although such VO₂⁺ species are rather common for vanadium(V) in aqueous systems [31,56–58].

The IR band due to the $\nu(\text{V}=\text{O})$ stretch vibration of VO(hebab) is observed at 952 cm^{-1} . This is within the usually observed range for six-coordinate vanadium(V) complexes [34,45]. The increased $\nu(\text{V}=\text{O})$ frequency, as compared to the VO(sabhea) complex (928 cm^{-1} [27]) of the corresponding Schiff base ligand, is consistent with the weaker tertiary amine nitrogen donor *trans* to the oxo moiety in the VO(hebab) complex. Consistent with the hydrogen bonding in the solid state the $\nu(\text{N}-\text{H})$ stretching vibration is observed at 3095 cm^{-1} . The Raman spectrum of a solid state sample of VO(hebab) shows the band of the $\nu(\text{V}=\text{O})$ stretching vibration at 950 cm^{-1} . In saturated DMF solution this band is shifted by 10 wavenumbers to higher energy, this might indicate a weakening of the *trans* vanadium to tertiary amine nitrogen bond in solution.

The deep red color of VO(hebab) in the solid state is consistent with an electronic transition at $19.5 \times 10^3 \text{ cm}^{-1}$ observed as a shoulder in the solid state UV-Vis reflection spectrum extending far into the visible region (up to $14 \times 10^3 \text{ cm}^{-1}$). This band is assigned to a ligand-to-metal charge-transfer (LMCT) transition on the basis of resonance Raman experiments. Due to the resonance Raman spectrum of

VO(hebab) this electronic transition is not related to just one specific vibrational mode, instead it is indicative of a rather delocalized electronic system. Enhanced bands in the resonance Raman spectrum are found in the region of 500 to 600 wavenumbers assigned to $\nu(\text{V-O})$ and $\nu(\text{V-N})$ stretching vibrations, at 951 cm^{-1} related to the $\nu(\text{V=O})$ stretching vibration, at 1285 cm^{-1} due to the $\nu(\text{O-C(aryl)})$ stretching vibration, and between 1500 and 1600 wavenumbers assigned to aromatic $\nu(\text{C=C})$ stretching vibrations. This result indicates contributions of the related ligand atoms to the HOMO of the VO(hebab) complex. In fact, density functional calculations [59] with the local spin density approximation in the parameterization given by Vosko et al. [60] confirm this assignment. The population analysis reveals large contributions from the atomic orbitals of the atoms O1, O2, N2 and C1–C6 (for notation see Fig. 3) to the HOMO, with the largest coefficient found for the $2p_z$ of the aryl oxygen O1. In contrast to the delocalized nature of the HOMO the LUMO is located at the vanadium center and predominantly composed of the $3d_{xy}$ atomic orbital. Both the theoretical results as well as the resonance Raman spectrum clearly indicate that the highest energy band in the electronic spectrum has to be assigned to a LMCT transition.

For the electronic absorption spectra in solution the situation is somewhat more complicated, since two isomeric forms of VO(hebab) coexist at different ratios depending on the solvent. This already is apparent from the color of the solutions obtained in different solvents like DMF or DMSO (yellow–orange) and chloroform (orange–red). In all three solvents the absorption bands are nearly invariant. The only significant difference is observed for the intensities of the two bands at about 23 and $28 \times 10^3\text{ cm}^{-1}$. As the extinction coefficient of the band at lower energy decreases in the series from chloroform to DMF and DMSO the other band at $28 \times 10^3\text{ cm}^{-1}$ is concomitantly increasing. According to ^{51}V NMR spectra the *cis*-ethoxide isomer becomes predominant as the solvent polarity increases (see Table 4). It is thus tempting to assign the two lowest energy bands to the LMCT transition of either of the two isomers observed in solution (*trans*-ethoxide at $23 \times 10^3\text{ cm}^{-1}$ and *cis*-ethoxide at $28 \times 10^3\text{ cm}^{-1}$, cf. Fig. 2).

4. Conclusions

A high-denticity pentadentate amine–phenol alkoxide ligand (H_3hebab) has been synthesized by reduction of the corresponding Schiff base compound. The VO^{3+} complex of the H_3hebab ligand was prepared by reaction with ammonium *meta*-vanadate in refluxing methanol. Crystallographic analysis of the VO(hebab) complex revealed that only the isomer with the oxo group in the *trans* position to the tertiary amine nitrogen is present in the solid state. The increased ligand flexibility, as compared to the Schiff base analogue, is evident from the varying stability of the two observed solution isomers, which is solvent dependent. The delocalized

nature of the HOMO of the VO(hebab) complex has been shown by resonance Raman spectroscopy as well as density functional calculations. In addition, the reaction of VO(hebab) with methanol and water has been investigated. This is of interest, since it might provide information on the stability of possible coordination environments of vanadium inside a protein and their chemical reactivity. In methanol VO(hebab) forms an adduct with presumably two molecules methanol which was only characterized by ^{51}V NMR, since the low formation constant did not permit other types of characterization. The hydrolysis studies of the VO(hebab) complex did not give any evidence for the formation of a VO_2^+ pervanadyl species, which on the other hand is rather common for vanadium(V) in aqueous systems. The implications of the BVS approach on the proposed model structures for the active site of the vanadium-dependent haloperoxidases are discussed. As a result the active site is expected either to possess a five-coordinate structure or a higher coordination with an electronically and/or sterically exceptional ligand environment.

5. Supplementary material

Further details of the crystal structure determination are available from the Fachinformationszentrum Karlsruhe, Gesellschaft für wissenschaftlich-technische Information mbH, D-76344 Eggenstein-Leopoldshafen (Germany), on quoting the depository number CSD-401 671, the name of the author and the journal citation.

Acknowledgements

The financial support of the Deutsche Forschungsgemeinschaft, the Fonds der Chemischen Industrie and the Herbert Quandt-Stiftung der VARTA AG is gratefully acknowledged. Thanks is due to Mrs B. Neumann for collecting the crystallographic data set. I thank Professor Dr A. Müller for his continued support.

References

- [1] N.D. Chasteen, *Vanadium in Biological Systems*, Kluwer, Dordrecht, 1990.
- [2] R. Wever and K. Kustin, *Adv. Inorg. Chem.*, 35 (1990) 81.
- [3] D. Rehder, *Angew. Chem.*, 103 (1991) 152.
- [4] A. Butler and C.J. Carrano, *Coord. Chem. Rev.*, 109 (1991) 61.
- [5] E. Bayer and H. Kneifel, *Z. Naturforsch., Teil B*, 27 (1972) 207.
- [6] H. Michibata and H. Sakurai, Vanadium in Ascidiaceans, in N.D. Chasteen (ed.), *Vanadium in Biological Systems*, Kluwer, Dordrecht, 1990, p. 153–171.
- [7] M.J. Gresser and A.S. Tracey, Vanadate as Phosphate Analogs in Biochemistry, in N.D. Chasteen (ed.), *Vanadium in Biological Systems*, Kluwer, Dordrecht, 1990, pp. 63–79.
- [8] J.L.C. Cantley, L. Josephson, R. Warner, M. Yanagisawa, C. Lechene and G. Guidotti, *J. Biol. Chem.*, 252 (1977) 7421.

- [9] Y. Schechter, J. Meyerovitsch, Z. Farfel, J. Sack, R. Bruck, S. Bar-Meir, S. Amir, H. Degani and S.D. Karlish, Insulin Mimetic Effects of Vanadium, in N.D. Chasteen (ed.), *Vanadium in Biological Systems*, Kluwer, Dordrecht, 1990, pp. 129–142.
- [10] R.L. Robson, R.R. Eady, T.H. Richardson, R.W. Miller, M. Hawkins and R.J. Postgate, *Nature*, 322 (1986) 388.
- [11] R.R. Eady, in W.J. Broughton and A. Pühler (eds.), *Nitrogen Fixation*, Vol. 4, Oxford University Press, London, 1986, pp. 1–49.
- [12] V.K. Shah, R.A. Vgalde, J. Imperial and W.J. Brill, *Am. Rev. Biochem.*, 53 (1984) 231.
- [13] H. Vilter, *Bot. Mar.*, 26 (1983) 429.
- [14] H. Vilter, *Bot. Mar.*, 26 (1983) 451.
- [15] H. Vilter, *Phytochem.*, 23 (1984) 1387.
- [16] E. de Boer, Y. van Kooyk, M.G.M. Tromp, H. Plat and R. Wever, *Biochim. Biophys. Acta*, 869 (1986) 48.
- [17] H. Plat, B.E. Krenn and R. Wever, *Biochem. J.*, 31 (1992) 2029.
- [18] J. Hornes, U. Kuetsgens, R. Chauvistre, W. Schreiber, N. Anders, H. Vilter, D. Rehder and C. Weidemann, *Biochim. Biophys. Acta*, 956 (1988) 293.
- [19] J.M. Arber, E. de Boer, C.D. Garner, S.S. Hasnain and R. Wever, *Biochemistry*, 28 (1989) 7968.
- [20] H. Vilter and D. Rehder, *Inorg. Chim. Acta*, 136 (1987) L7.
- [21] D. Rehder, H. Holst, W. Priebsch and H. Vilter, *J. Inorg. Biochem.*, 41 (1991) 171.
- [22] E. de Boer, K. Boon and R. Wever, *Biochemistry*, 27 (1988) 1629.
- [23] E. de Boer, C.P. Keijzers, A.A.K. Klaassen, E.J. Reijerse, D. Collison, C.D. Garner and R. Wever, *FEBS Lett.*, 235 (1988) 93.
- [24] K. Knüttel, A. Müller, D. Rehder, H. Vilter and V. Wittneben, *FEBS Lett.*, 302 (1992) 11.
- [25] J.H. Dawson, *Science*, 240 (1988) 433.
- [26] S. Liu, L. Gelmini, S.J. Rettig, R.C. Thompson and C. Orvig, *J. Am. Chem. Soc.*, 114 (1992) 6081.
- [27] W. Plass, *Z. Anorg. Allg. Chem.*, 620 (1994) 1635.
- [28] Space Group Symmetry, in T. Hahn (ed.), *International Tables for Crystallography*, Vol. A, Kluwer, Dordrecht, 4th edn., 1995.
- [29] G.M. Sheldrick, *SHELXTL PLUS Crystallographic System*, Siemens Analytical X-ray Instruments, Inc., Madison, WI, 1989.
- [30] G.M. Sheldrick, *SHELXL-93*, University of Göttingen, Germany, 1993.
- [31] G.J. Colpas, B.J. Hamstra, J.W. Kampf and V.L. Pecoraro, *Inorg. Chem.*, 33 (1994) 4669.
- [32] C.J. Carrano, M. Mohan, S.M. Holmes, R. de la Rosa, A. Butler, J.M. Charnock and C.D. Garner, *Inorg. Chem.*, 33 (1994) 646.
- [33] W.R. Scheidt, *Inorg. Chem.*, 12 (1973) 1758.
- [34] J.C. Dutton, K.S. Murray and E.R.T. Tiekink, *Inorg. Chim. Acta*, 166 (1989) 5.
- [35] D.C. Fisher, S.J. Barclay-Peet, C.A. Balfe and K.N. Raymond, *Inorg. Chem.*, 28 (1989) 4399.
- [36] K. Nakajima, M. Kojima, K. Toriumi, K. Saito and J. Fujita, *Bull. Chem. Soc. Jpn.*, 62 (1989) 760.
- [37] W. Banske, E. Ludwig, E. Uhlemann, F. Weller, K. Dehnicke and W. Herrmann, *Z. Anorg. Allg. Chem.*, 613 (1992) 36.
- [38] E. Ludwig, H. Hefele, U. Schilde and E. Uhlemann, *Z. Anorg. Allg. Chem.*, 620 (1994) 346.
- [39] H.H. Thorp, *Inorg. Chem.*, 31 (1992) 1585.
- [40] I.D. Brown, The Bond-Valence Method: An Empirical Approach to Chemical Structure and Bonding, in M. O'Keefe and A. Navrotsky (eds.), *Structure and Bonding in Crystals*, Vol. 2, Academic Press, New York, 1981.
- [41] M. O'Keefe, *Struct. Bonding (Berlin)*, 71 (1989) 161.
- [42] I.D. Brown and D. Altermatt, *Acta Crystallogr., Sect. B*, 41 (1985) 244.
- [43] L. Banci, A. Bencini, A. Dei and D. Gatteschi, *Inorg. Chim. Acta*, 84 (1984) L11.
- [44] A.A. Diamantis, J.M. Frederiksen, M.A. Salam, M.R. Snow and E.R.T. Tiekink, *Aust. J. Chem.*, 39 (1986) 1081.
- [45] X. Li, M.S. Lah and V.L. Pecoraro, *Inorg. Chem.*, 27 (1988) 4657.
- [46] V.L. Pecoraro, *Inorg. Chim. Acta*, 155 (1989) 171.
- [47] C.J. Carrano, C.M. Nunn, R. Quan, J.A. Bonadies and V.L. Pecoraro, *Inorg. Chem.*, 29 (1990) 944.
- [48] S. Holmes and C.J. Carrano, *Inorg. Chem.*, 30 (1991) 1231.
- [49] J. Chakravarty, S. Dutta, S.K. Chandra, P. Basu and A. Chakravorty, *Inorg. Chem.*, 32 (1993) 4249.
- [50] M.J. Clague, N.L. Keder and A. Butler, *Inorg. Chem.*, 32 (1993) 4754.
- [51] C.R. Cornman, G.J. Colpas, J.D. Hoeschele, J. Kampf and V.L. Pecoraro, *J. Am. Chem. Soc.*, 114 (1992) 9925.
- [52] C.R. Cornman, J. Kampf and V.L. Pecoraro, *Inorg. Chem.*, 31 (1992) 1983.
- [53] D. Rehder, C. Weidemann, A. Duch and W. Priebsch, *Inorg. Chem.*, 27 (1988) 584.
- [54] D. Rehder, Biological Applications of ^{51}V NMR Spectroscopy, in N.D. Chasteen (ed.), *Vanadium in Biological Systems*, Kluwer, Dordrecht, 1990, pp. 173–197.
- [55] J. Mason (ed.), *Multinuclear NMR*, Plenum, New York, 1987.
- [56] D.C. Crans, H. Chen, O.P. Anderson and M.M. Miller, *J. Am. Chem. Soc.*, 115 (1993) 6769.
- [57] D.C. Crans and K.P. Shin, *J. Am. Chem. Soc.*, 116 (1994) 1305.
- [58] A. Butler, The Coordination and Redox Chemistry of Vanadium in Aqueous Solution, in N.D. Chasteen (ed.), *Vanadium in Biological Systems*, Kluwer, Dordrecht, 1990, pp. 25–49.
- [59] *ADF 1.1.3*, Department of Theoretical Chemistry, Vrije Universiteit, Amsterdam, 1994; E.J. Baerends, D.E. Ellis and P. Ros, *Chem. Phys.*, 2 (1973) 41; G. te Velde and E.J. Baerends, *J. Comp. Phys.*, 99 (1992) 84.
- [60] S.H. Vosko, L. Wilk and M. Nusair, *Can. J. Phys.*, 58 (1980) 1200.